Journal of Medicinal Chemistry

Article

pubs.acs.org/jmc

Aromatic Bis-*N*-hydroxyguanidinium Derivatives: Synthesis, Biophysical, and Biochemical Evaluations

Amila Kahvedžić,[†] Seema-Maria Nathwani,[‡] Daniela M. Zisterer,[‡] and Isabel Rozas*[,†]

[†]School of Chemistry, Trinity Biomedical Science Institute, Trinity College Dublin, 154-160 Pearse Street, Dublin 2, Ireland

[‡]School of Biochemistry and Immunology, Trinity Biomedical Science Institute, Trinity College Dublin, 154-160 Pearse St., Dublin 2, Ireland

Supporting Information

ABSTRACT: In this paper we report the synthesis of a new family of hydroxyguanidinium aromatic derivatives (**4a**–**g**) as potential minor groove binders and cytotoxic agents. Their DNA affinity was evaluated by thermal denaturation experiments using salmon sperm DNA. The antiproliferative effects of derivatives **4a**, **4d**, and **4f** were evaluated in human promyelocytic HL-60, breast carcinoma MCF-7, and neuroblastoma Kelly cell lines using the AlamarBlue viability assay, and IC_{50} values were obtained. All three compounds were active in the HL-60 cell line. In particular, **4b** exhibits antiproliferative effects in all three cell lines while **4d** reduced HL-60 and Kelly viability. Both **4b** and **4d** produced considerable antiproliferative activity in the Kelly cell line. Derivative **4d** was chosen for further cell cycle and apoptosis studies using flow cytometric analysis of cellular DNA content.

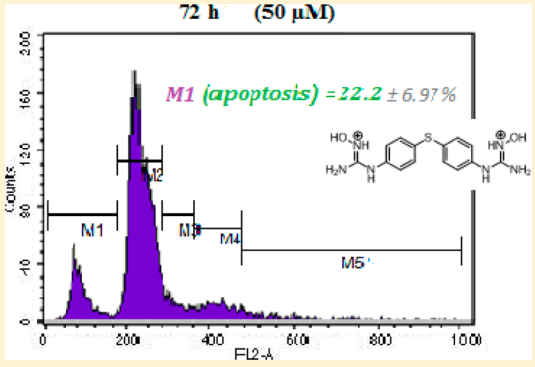

INTRODUCTION

According to the World Health Organisation, 7.6 million people died from cancer in 2008 and this rate is expected to increase to 13.1 million by 2030.[1] Although some advances in treatment have been made,[2,3] there remains a need for more efficient therapies. Minor groove binding agents are associated with antiproliferative properties, disrupting the DNA replication process by interfering with DNA replicative enzymes such as topoisomerases,[4] subsequently leading to programmed cell death (apoptosis). During the past 5 years we have prepared a number of symmetric and asymmetric guanidinium and 2-aminoimidazolinium derivatives that have been shown to be DNA minor groove binders (MGBs). All these compounds contain two cationic terminal ends, two phenyl rings, in a para–para arrangement, connected by a linker. Relevant biophysical measurements such as DNA thermal melting, circular dichroism (CD), and isothermal calorimetry (ITC) confirmed binding and affinity toward the minor groove.[5−7] These encouraging results led us to explore new families of potential DNA MGBs including isouronium derivatives.[8]

Continuing our search for more efficient MGBs, we have designed and synthesized a novel hydroxyguanidinium-based family with the aim of achieving anticancer activity by inducing apoptotic cell death. The hydroxyguanidinium cation combines the features of guanidine (associated with DNA binding) and hydroxyurea (readily enters the cell and disrupts ribonucleotide incorporation[9]) and consequently combines DNA binding and antitumor properties. Hence, the incorporation of the hydroxyguanidinium motif to the basic structure of those MGBs previously prepared by us would further allow the investigation of the nature of the cationic moiety. First, the additional hydroxyl group can act simultaneously as a hydrogen bond (HB) donor and acceptor and this would potentially introduce an extra point of interaction, improving binding in the minor groove (Figure 1). Second, its lower basicity, relative to that of the guanidinium or 2-aminoimidazolinium cations previously used, would provide an interesting comparison in terms of pharmacokinetic properties.

The hydroxyguanidinine group occurs naturally in a plethora of enzymatic pathways, and compounds with this group exhibited cytotoxic activity in cancers such as Novikoff hepatoma and Walker 256 carcinosarcoma.[10] Indeed, studies by Young et al. have demonstrated that hydroxyguanidine derivatives inhibit DNA synthesis.[11] Interestingly, it has been reported that pentamidine and furamidine hydroxylated derivatives, synthesized as anti-trypanasomal agents, showed activity by oral and intravenous routes with the bis-hydroxypentamidine derivative being as active but less potent than its parent molecule in experimental mice.[12,13]

Taking all this into consideration, this paper describes the preparation of a new bis-*N*-hydroxyguanidine family, their DNA binding measured by DNA thermal denaturation experiments. In addition, the cytotoxicity of selected derivatives toward promyelocytic HL-60, breast carcinoma MCF-7, and neuroblastoma Kelly human cancer cell lines is presented along with the effects on apoptosis.

Received: September 19, 2012
Published: December 20, 2012

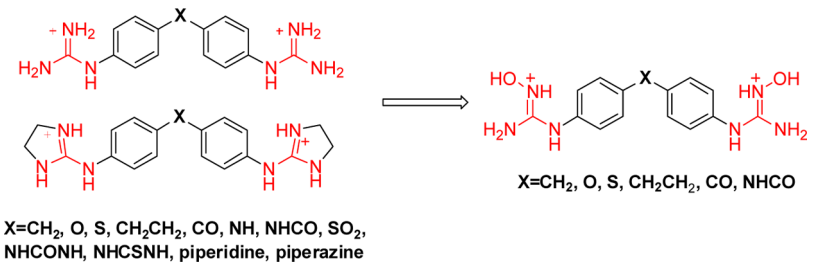

Figure 1. Bis-guanidinium and bis-2-aminoimidazolinium derivatives previously prepared by Rozas and co-workers (left) and *N*-hydroxyguanidiniums prepared in this work (right).

Scheme 1. Synthesis of Aromatic Hydroxyguanidines As Described by Martin et al.[14]

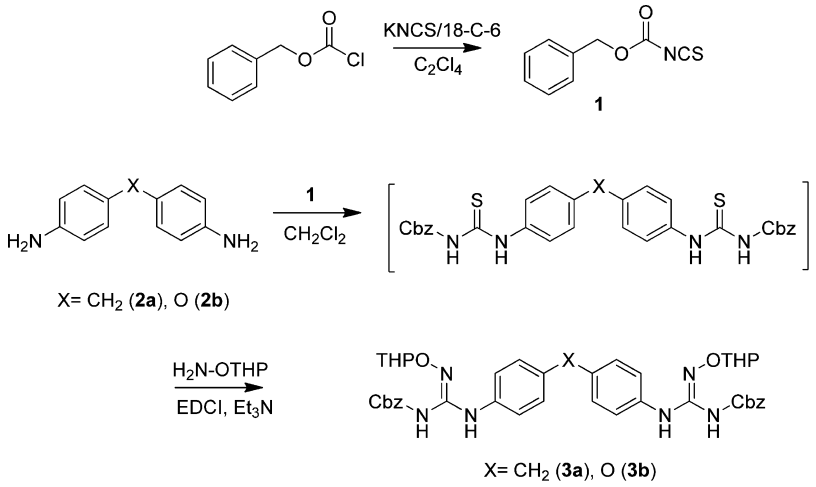

Scheme 2. Simultaneous Deprotection Reaction for Compounds 3a and 3b To Yield the Corresponding Hydrochloride Salts 4a and 4b

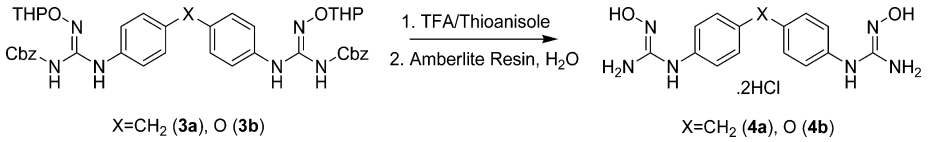

RESULTS AND DISCUSSION

Chemistry. There are several synthetic routes to generate the hydroxyguanidinium moiety reported in the literature, and we followed in particular that described by Martin et al.,[14] involving the transformation of an amino group to an active thiourea, followed by the reaction with a protected hydroxylamine and a suitable deprotection reaction. Preparation of the thiourea intermediate requires the synthesis of the carbamoyl isothiocyanate (**1**), which involves the reaction of benzyl chloroformate with KNCS in the presence of 18-crown-6 in anhydrous tetrachloroethylene (Scheme 1). Martin et al. reported decomposition to the benzyl thiocyanate when purification was attempted by distillation or silica gel chromatography; hence, when we performed this synthesis, no purification was carried out. Therefore, once product **1** was prepared, following this pathway, identified, and analyzed by ^{1}H NMR, it was dissolved in dry DCM to give a final 0.5 M stock solution to be stored at 4 °C. The reaction of amines with carbamoyl isothiocyanates to yield thioureas has been shown to proceed efficiently and in high yield by using the activating agent ECDI.[15,16] Hence, a stock solution of **1** was used to react with appropriate starting amines (**2a** and **2b** in Scheme 1) to form the corresponding thioureas. These can be isolated or used directly to react with a protected hydroxylamine, generating the required hydroxyguanidinium moiety. Following this synthetic approach the corresponding −CH_2− (**3a**) and −O− (**3b**) bis-derivatives were prepared and fully characterized. Attempts were made with other diamines with linkers such as −CH_2CH_2− (**2c**), −S− (**2d**), −CO− (**2e**), and −NHCO− (**2f**); however, the reactions failed because of the highly inactive nature of these starting diamines.

The −CH_2- and −O-linked protected hydroxyguanidinium derivatives (**3a,b**) were deprotected using the conditions described by Kiso et al.[17] to generate the corresponding trifluoroacetate salts (Scheme 2) using a 10:1 mixture of TFA/thioanisole to cleave both the THP and Cbz protecting groups in a concerted manner. Finally, the trifluoroacetate salts were treated with an Amberlite exchange resin in water overnight to form the hydrochloric salts (**4a** and **4b**).

The problems found for the synthesis of the other diaromatic hydroxyguanidines could be accounted not only for the deactivated nature of the diaromatic starting amines but also for the problematic CbzNCS synthesis. Therefore, an alternative strategy in the synthesis of the hydroxyguanidiniums, involving the generation of cyanamide intermediates, was searched. Cyanogen bromide is the most commonly used

dx.doi.org/10.1021/jm301358s | J. Med. Chem. 2013, 56, 451−459

reagent in the generation of cyanamides for the synthesis of hydroxyguanidines.[18−20] In particular, Xian et al.[21] reported a method for the preparation of cyanamides using amines and CNBr with TEA and DCM; however, for primary amines like our starting compounds the modified procedure of Pankratov et al.[22] is recommended using dimethylacetamide (DMAA) as both a solvent and acceptor of the liberated HBr. Thus, a solution of the corresponding starting diamine in DMAA was added dropwise to a solution of CNBr in anhydrous DMAA at room temperature. The mixture was heated to 35 °C and stirred overnight under argon. Following this method, the corresponding $-CH_2-$, −O-, $-CH_2CH_2-$, −S-, −CO-, and −NHCO-linked cyanamides (**5a−f**) along with phenylcyanamide (**5g**) were successfully prepared in moderate to good yields (Scheme 3) and fully characterized.

Scheme 3. Preparation of Cyanamides 5a−f

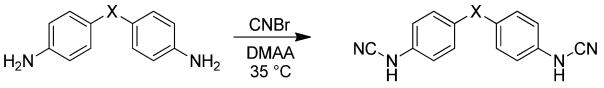

X= CH_2 (**5a**), O (**5b**), CH_2CH_2 (**5c**), S (**5d**), CO (**5e**), CONH (**5f**)

After the cyanamide intermediates were synthesized, the next step was the generation of the hydroxyguanidinium derivatives. Considering the high reactivity[23] and low stability[24] of these compounds and their sensitivity to heat and moisture,[25,26] we utilized them without further purification in the remainder of the hydroxyguanidinium synthesis. The optimized conditions for the preparation of the proposed hydroxyguanidines (Scheme 4) involved the use of a sealed reaction vessel with hydroxylamine (dried under vacuum at 40 °C) and K_2CO_3 in excess, the cyanamides flushed with argon, and 4 Å molecular sieves. Then anhydrous EtOH was added dropwise and the mixture was allowed to stir overnight at room temperature.

Considering that hydroxyguanidines can decompose at room temperature,[26,27] they were converted to hydrochlorides for storage and further use. This conversion was achieved by treating the crude mixture with excess 1 M HCl/ether solution overnight at room temperature followed by solvent removal under vacuum to yield a crude salt mixture which was purified by reverse-phase chromatography using H_2O/MeCN. Thus, the $-CH_2-$, −O-, $-CH_2CH_2-$, −S-, −CO-, and −NHCO-linked derivatives (**4a−f**) and the phenylhydroxyguanidinium derivative (**4g**) were prepared (Scheme 4) and stored at −20 °C.

Biophysical Studies. To determine the DNA affinity of all the bis-hydroxyguanidinium hydrochlorides prepared (compounds **4a−f**), thermal denaturation experiments were performed. Salmon sperm DNA (wild-type, sequence unspecific oligonucleotide) was used and its melting temperature (T_m) determined to be 68 °C. To evaluate the binding strength of the hydroxyguanidiniums, a 15 μM solution of each compound was prepared and added to DNA (150 μM) so that a final P/D ratio of 10 was achieved. The experiment was then performed, and a characteristic plot and corresponding T_m value were obtained for each DNA/ligand complex. The results for compounds **4a−f** were obtained in at least two independent experiments and are presented in Table 1.

Table 1. DNA Thermal Denaturation Assay Results for the Bis-hydroxyguanidinium Family and the Bis-guanidinium Analogues

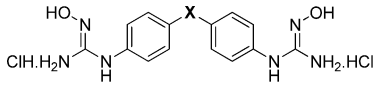

compd (X)	ΔT_m (°C)[a]	bis-guanidinium derivative	ΔT_m (°C)[b]	ΔT_m (°C)[c]
4a (CH_2)	0	CH_2	8	18.8
4b (O)	1	O		22.1
4c (CH_2CH_2)	0	CH_2CH_2		26.1
4d (S)	1	S		20.1
4e (CO)	0	CO	4	27.6
4f (NHCO)	1	NHCO	11	40.1

[a]Using salmon sperm DNA. This work. [b]Using salmon sperm DNA. Previously obtained by Rozas and co-workers.[27] [c]Using poly(dA·dT)$_2$. Previously obtained by Rozas and co-workers.[5,28]

In general, all the derivatives possess very poor DNA affinity with ΔT_m values of 0−1 °C. Considering the range of linker groups used in this family, with differences in polarity and geometry, these results suggest that the linker has no effect on DNA binding. This is in agreement with the crystal structure of the related −NH-linked bis-2-aminoimidazolinium analogue bound to 5′-d(CTTAATTCGAATTAAG),[29] which shows the −NH− linker pointing outside of the groove and hence not contributing to the binding.

Additionally, our results correlate to those reported for *N,N′*-dihydroxypentamidine. Although proving to be as active (but not as potent) as pentamidine in antitrypanosomal assays,[12] the hydroxy derivative was found to be a poor MGB (ΔT_m = 0.2 °C) compared to pentamidine (ΔT_m = 10.7 °C).[30] Thus, N-hydroxylation of pentamidine resulted in an almost complete loss of binding ability similar to what has been observed in this work when comparing with the corresponding bis-guanidinium derivatives previously prepared by us[5,6,30] (see Table 1).

We have reported that that the introduction of the hydroxyl group in the guanidinium moiety (pK_a = 13.7)[31] lowers the pK_a of the resulting hydroxyguanidinium derivatives ($pK_a \approx 8-11$; Table 2);[32] therefore, the hydroxyguanidinium, being less basic, is not as readily ionized and hence may not have the same strong attraction toward the negative minor groove. Thus, the DNA affinity of hydroxyguanidiniums, despite having additional points for HB interactions, is undermined by the less basic nature of the cationic moiety itself.

Biochemical Results. *Viability Assays.* The antiproliferative effects of the hydroxyguanidinium family prepared in this

Scheme 4. Synthesis of the Hydroxyguanidine Hydrochloride Salts 4a−f

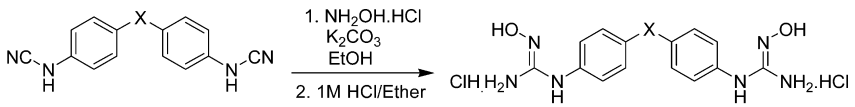

X= CH_2 (**4a**), O (**4b**), CH_2CH_2 (**4c**), S (**4d**), CO (**4e**), NHCO (**4f**)

dx.doi.org/10.1021/jm301358s | J. Med. Chem. 2013, 56, 451−459

Table 2. IC_{50} Values Calculated for the Hydroxyguanidinium Derivatives in the HL-60, MCF-7, and Kelly Cell Lines[a]

Structure	pK_a	HL-60 (μM)	MCF-7 (μM)	Kelly (μM)
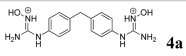 **4a**	-	72.8 ±4.8	>100	-
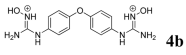 **4b**	8.3 10.9[40]	65.5 ±10.7	36.2 ±7.9	11.7 ±0.6
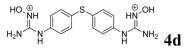 **4d**	-	47.7 ±6.0	>100	8.9 ±1.0
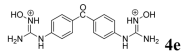 **4e**	-	>100	-	-
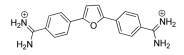 **Furamidine**	10.4 11.8[41]	87.5 ±2.3	92.8 ±6.7	27.4 ±5.1

[a]The pK_a values for compound **4b** and furamidine are included for comparative purposes.

study were evaluated using the AlamarBlue viability assay[33,34] on selected cancer cell lines derived from both the hematopoietic system and solid tumors. In addition, the ability of the lead derivatives to induce apoptosis was investigated using flow cytometry.

First, the human Caucasian promyelocytic leukemia cell line HL-60 was utilized. This is a well-established cell line used as an in vitro model for the study of myeloid growth and differentiation.[35,36]

Stock concentrations of the bis-hydroxyguanidiniums **4a**, **4b**, **4d**, and **4e** and furamidine (used as reference) were prepared in water. A range of concentrations of each derivative was assessed in triplicate in at least three independent experiments. Results were analyzed accordingly, and mean values with standard error with respect to vehicle control were obtained (Figure 2). A clear relationship between drug concentration and AlamarBlue reduction was established.

The corresponding IC_{50} values were calculated (Table 2) showing that three of these compounds reduced HL-60 viability. The best derivative was found to be the −S-linked compound (**4d**), while the $-CH_2-$ and −O-linked hydroxyguanidinium derivatives (**4a** and **4b**) were slightly less active. The remaining derivative, the −CO-linked **4e**, produced no activity at the highest concentration tested. Interestingly, furamidine displayed similar activity to our active derivatives with an IC_{50} of 77.6 ± 1.15 μM.

From these results some structure−activity relationships can be extracted. First, the fact that these compounds will be fully protonated at pH 7.4 (see pK_a values for compound **4b** in Table 2) will not affect their cell permeation, since it has been proposed that dicationic compounds such as furamidine take advantage of polyamine and guanidine transporter systems into the cell.[37] Second, although the inhibitory values obtained for compounds **4a**, **4b**, and **4d** are not better than those previously obtained for our bis-guanidinium-like derivatives,[38] their consistency suggests the idea that the hydroxyguanidinium functionality is an active motif.

In theory, the compounds that most tightly bind into the groove should interfere with DNA replication most effectively eliciting the strongest anticancer effects through processes such as apoptosis. However, the poor DNA thermal melting results (Table 1) suggest that antiproliferative effects are being induced irrespective of their binding ability. This is also the case with furamidine, which, although known to bind exceptionally well to the minor groove [ΔT_m = 26.2 using poly(dA-dT)$_2$],[39] shows only moderate antiproliferative activity, poorer than most of our derivatives. This may suggest that such compounds elicit their effects by an alternative mode of action.

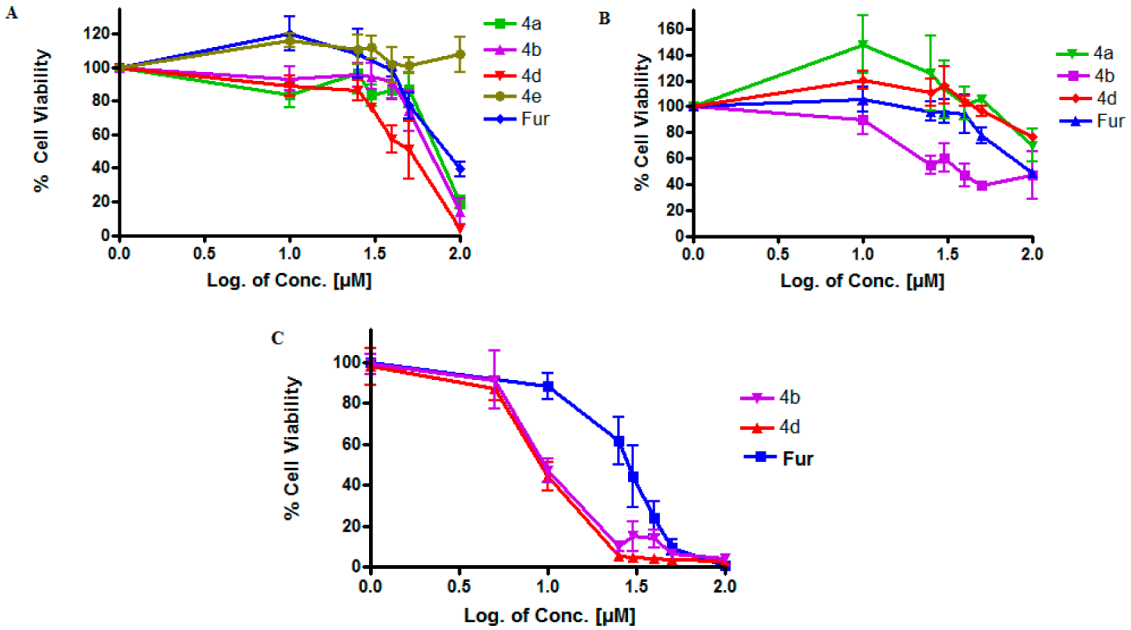

Figure 2. Effects of bis-hydroxyguanidiniums (**4a,b,d,e**) on the viability of HL-60 (A), MCF-7 (B), and Kelly (C) cells as determined by AlamarBlue viability assays. Cells were seeded at a density of 4×10^4, 1×10^4, and 6×10^3 cells per well, respectively, onto a 96-well plate and treated with vehicle alone (1% (v/v), ddH_2O, or the compounds at 1−100 μM. Furamidine (Fur) was used as a reference and tested in the same manner. Cells were incubated for 72 h at 37 °C, after which they were treated with 10% (v/v) AlamarBlue and left in darkness in an incubator for 4.5 h. The resulting fluorescence was read using a plate reader from which percentage viability was calculated. The points on the graph represent mean values ± SEM from at least three independent experiments performed in triplicate.

dx.doi.org/10.1021/jm301358s | J. Med. Chem. 2013, 56, 451−459

Table 3. Effects of 4d on the Cell Cycle Profile of HL-60 Cells[a]

compd (50 μM)	M1 (pre-G_1)	M2 (G_0/G_1)	M3 (S)	M4 (G_2/M)	M5 (G_n)
24 h, vehicle	0.81 ± 0.11	56.05 ± 1.40	24.46 ± 1.15	16.73 ± 0.59	2.96 ± 0.79
24 h, **4d**	1.53 ± 0.28	55.9 ± 0.57	25.85 ± 2.23	14.57 ± 1.62	2.35 ± 0.98
48 h, vehicle	1.41 ± 0.32	58.77 ± 2.33	24.29 ± 1.37	11.35 ± 1.05	3.02 ± 0.56
48 h, **4d**	6.44 ± 1.55	56.62 ± 6.66	21.71 ± 6.29	10.78 ± 0.39	1.94 ± 0.14
72 h, vehicle	2.21 ± 0.57	59.5 ± 1.50	23.58 ± 1.38	10.53 ± 0.81	3.43 ± 0.48
72 h, **4d**	22.2 ± 6.97	44.8 ± 11.13	15.99 ± 4.70	14.54 ± 5.67	2.1 ± 0.33

[a]Cells were treated with vehicle (ddH_2O) or 50 μM compound and analyzed by flow cytometry as described in the text and Experimental Section. Mean values ± SEM of the proportion of cells of each phase of the cell cycle from at least three independent experiments are shown with M1 = pre-G_1 (<2N DNA), M2 = G_0/G_1 (2N DNA), M3 = S (2N−4N DNA), M4 = G_2/M (4N DNA), and M5 = G_n (>4N DNA). Percentage apoptosis is determined from the M1 (pre-G_1) peak.

Those derivatives that showed the best activity in HL-60 cells (**4a**, **4b**, and **4d**) were tested on two additional cancer cell lines representative of solid tumors: MCF-7 (human breast carcinoma) and Kelly (human neuroblastoma). The relationship between AlamarBlue fluorescence and cell number was found to be directly proportional in all the assays. All compounds were assessed in triplicate in at least three independent experiments. The same test concentrations as for the HL-60 assays were used for each compound (a $^1/_{100}$ dilution was made with final concentrations of 10−100 μM), and 1% (v/v) doubly distilled H_2O (ddH_2O) was used as a vehicle control. Prism Graphpad was used to analyze the results which were obtained as mean ± SEM values (Figure 2).

The results of the viability assays indicate that these compounds displayed a lower spectrum of activity in MCF-7 cells than in HL-60 and in Kelly cells. The −O-linked derivative **4b** proved to be the most potent with an average of 53% viability reduction at 100 μM and a corresponding IC_{50} of 45.2 μM (Figure 2 and Table 2). Derivatives **4a** and **4d** reduced viability by 29.8% and 23.1%, respectively, at the same concentration. Despite the lower spectrum of activity observed in MCF-7 cells, furamidine was found to be considerably less potent than **4b** in the inhibition of viability (Table 2).

In comparison to the HL-60 cell line, the lowest IC_{50} value was observed for compound **4b**. As before, no direct correlation between minor groove binding and antiproliferative activity was evident. In fact, **4b**, which has been shown to be a weak MGB, was found to be more potent than furamidine. Further screening of a larger family of compounds would have to be carried out in order to identify possible pharmacophoric elements for this cell line.

Compounds **4b** and **4d** that gave the best results in MCF-7 cells were also evaluated on the Kelly (human neuroblastoma) cell line. Neuroblastoma is the most common extracranial solid tumor in childhood,[42] and therefore, there is a compelling demand for new treatments. After 72 h of treatment, viability results (Figure 2) and corresponding IC_{50} values (Table 2) were obtained and analyzed. As can be seen from Figure 2, encouraging inhibition of Kelly cells was observed with **4b** and **4d**, surprisingly, the best results obtained among the three cell lines. Compound **4d** showed a potent inhibition of viability across the concentration range with, on average, 96.8%, 95%, 93.9%, and 79.4% reduction in viability at 100, 50, 40, and 30 μM (four independent experiments). Alternatively, **4b** also exhibited potent activity with average values of 95.8%, 89.9%, 86.4%, and 76.2% at the same concentrations. In comparison, furamidine showed lower potency. The corresponding IC_{50} values are presented in Table 2. The results obtained suggest that the hydroxyguanidinium motif is beneficial to the antiproliferative effect in Kelly cells. As mentioned previously, this may be attributed to the low basicity of this cation. A larger library of compounds would have to be tested in order for this to be confirmed.

Overall, a spectrum of viability inhibition was observed among the hydroxyguanidinium series in the HL-60, MCF-7, and Kelly cell lines, suggesting that these derivatives hold potential as anticancer agents. As can be seen in Table 2, three of the four derivatives (**4a**, **4b**, and **4d**) produced some activity in at least one cell line. The most active derivative was the −O-linked **4b**, which exhibited activity in all three cell lines. This was followed by the −S-linked **4d**, which was active in the HL-60 and Kelly cell lines but inactive in the MCF-7 cell line up to 100 μM. Particular attention should be paid to the results obtained in the Kelly cell line since, as previously mentioned, there is a compelling demand for new therapies to treat neuroblastoma.

As mentioned throughout, all the derivatives tested were found to be more potent in terms of cell viability inhibition than furamidine. Looking at the values obtained for this known MGB with the HL-60, MCF-7, and Kelly cell lines (77.6, 97.4, and 28 μM, respectively) in the present work reveals that our compounds hold potential as anticancer agents and should be investigated further. To the best of our knowledge, no previous IC_{50} values for furamidine in these cell lines have been published.

Flow Cytometry. The antiproliferative results obtained only indicate the effects on growth and proliferation and do not discriminate between cell cycle arrest and/or induction of cell death. Therefore, flow cytometric analysis was carried out on **4d** treated HL-60 cells, this compound being chosen as a suitable representative of the bis-hydroxyguanidinum family. Flow cytometry allows the evaluation of the populations of cells in different stages of the cell cycle and hence allows the determination of the amount of cells undergoing apoptosis (pre-G_1 peak).

For the flow cytometric studies on compound **4d**, HL-60 cells were seeded at a density of 2×10^5 cells mL^{-1} in RPMI medium and treated with vehicle (ddH_2O) or 50 μM compound and left to incubate at 37 °C for up to 72 h. Cells were subsequently fixed in ice-cold 70% EtOH/PBS and left at −20 °C for overnight fixation. Samples were then centrifuged, and the resulting cell pellets were resuspended in PBS. Each sample was then treated first with RNase and then with propidium iodide (PI).

The values presented in Table 3 are obtained from recorded plots (increasing amounts of DNA versus number of cells detected) that consist of a series of peaks for each sample of treated and untreated cells. In this case, 10 000 cells were

dx.doi.org/10.1021/jm301358s | J. Med. Chem. 2013, 56, 451−459

monitored per experiment. Accordingly, each peak indicates the proportion of cells in a particular phase of the cell cycle: M1 (pre-G_1), M2 (G_0/G_1 phase), M3 (synthesis phase), M4 (G_2/M phase), and M5 (polyploid). Apoptotic cells have a low DNA content and will appear in the M1 peak. With this in mind, mean ± SEM results were calculated from three independent experiments.

The results in Table 3 show that derivative **4d** induced apoptosis in HL60 cells in a time-dependent manner. At the 24 h time-point, it is evident that the compound has very little effect on HL-60 cell viability and proliferation. This is indicated by the low proportion of cells in the apoptotic M1 peak (1.53 ± 0.28%) which is very close to that of the vehicle (0.81 ± 0.11%). Correspondingly, the proportion of cells in the alternative M2−M5 phases is analogous to the vehicle control. This suggests that **4d** requires a longer period of time to exert its effects on the HL-60 cells. Analysis of the M1 (pre-G1) peak at 48 h shows that **4d** induced only a modest extent of apoptosis with 6.44 ± 1.55% cells in pre-G_1 in comparison to 1.41 ± 0.32% of the vehicle. In general, however, significant changes have not occurred and most values are comparable to those of the vehicle.

The most statistically significant changes are evident after 72 h of incubation with increased apoptosis occurring at this time (Figure 3). Approximately a fifth (22.2 ± 6.97%) of the cell

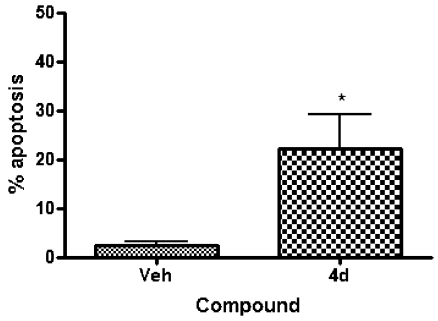

Figure 3. Apoptosis induction by **4d** in the HL-60 cell line as determined by flow cytometric analysis after 72 h. Cells were seeded at a density of 2×10^5 cells mL^{-1} and treated with 50 μM **4d**. Aliquots were collected at 72 h and treated as described in the Experimental Section. Values are representatives of the mean ± SEM from at least three independent experiments: (*) $P < 0.05$ (as determined by unpaired t test).

population has undergone apoptosis in comparison to 2.21 ± 0.57% in vehicle treated cells, and the proportion of cells in M2−M5 has likewise been reduced.

CONCLUSIONS

We have described the design and synthesis of a new hydroxyguanidinium family by means of two synthetic routes. The first involved the generation of an active thiourea intermediate from an isothiocyanate yielding derivatives **4a** and **4b**. A second synthetic route was used involving the transformation of an amino group into a cyanamide intermediate using CNBr. These cyanamides (**5a−f**) were then reacted with hydroxylamine hydrochloride in the presence of K_2CO_3, and the resulting hydroxyguanidines were subsequently converted to their hydrochlorides salts **4a−f**.

These derivatives were evaluated as MGBs by DNA thermal denaturation assays using salmon sperm DNA. Unfortunately, poor results were obtained with ΔT_m values of 0−1 °C, indicating that the hydroxylamine functionality penalizes DNA binding.

The antiproliferative effects (IC_{50} values) of derivatives **4a**, **4b**, **4d**, and **4e** were evaluated in the HL-60, MCF-7, and Kelly cancer cell lines using the AlamarBlue cell viability assay with furamidine as a control. Three derivatives were active in the HL-60 cell line (**4a**, **4b**, and **4d**) with IC_{50} values of 46.4−71.3 μM. Only **4b** was found to be active against the MCF-7 cells at the chosen concentration range (IC_{50} = 45.2 μM), while in the Kelly cells, derivatives **4b** and **4d** produced the lowest IC_{50} values (12.2 and 8.6 μM, respectively) among the three cell lines. Furamidine was found to be less potent and produced poorer IC_{50} values than our compounds in all three cell lines.

Flow cytometry allowed the further study of the effects of **4d** in terms of cell cycle events and apoptotic activity. HL-60 cells were treated with the compound and analyzed at 24, 48, and 72 h. Cytotoxic effects were mostly observed at 72 h with approximately a fifth of the cells undergoing apoptosis. No other significant cell cycle effects were observed.

From the results obtained, no direct correlation between DNA binding and biological effect can be established. Hence, these compounds may function by an alternative mode of action. Further studies would have to be performed to investigate their exact target. Overall, hydroxyguanidinium-based derivatives display a spectrum of cytotoxic activity, and in particular, special attention should be paid to the results obtained by **4b** and **4d** in the neuroblastoma Kelly cell line.

EXPERIMENTAL SECTION

Chemistry. All commercial chemicals were obtained from Sigma-Aldrich or Fluka and were used without further purification. Deuterated solvents for NMR use were purchased from Apollo. Dry solvents were prepared using standard procedures, according to Vogel, with distillation prior to use. Chromatographic columns were run using silica gel 60 (230−400 mesh ASTM). Solvents for synthetic purposes were used at GPR grade. Analytical TLC was performed using Merck Kieselgel 60 F_{254} silica gel plates. Visualization was by UV light (254 nm). NMR spectra were recorded in a Bruker DPX-400 Avance spectrometer, operating at 400.13 and 600.1 MHz for ^{1}H NMR and 100.6 and 150.9 MHz for ^{13}C NMR. Shifts are referenced to the internal solvent signals. NMR data were processed using Bruker Win-NMR 5.0 software. Electrospray mass spectra were recorded on a Mass Lynx NT V 3.4 on a Waters 600 controller connected to a 996 photodiode array detector with methanol as carrier solvent. Melting points were determined using an Electrothermal IA9000 digital melting point apparatus and are uncorrected. The purity of the target compounds (all ≥95%) has been evaluated by elemental analyses (carried out at the Microanalysis Laboratory, School of Chemistry and Chemical Biology, University College Dublin, Ireland) all of which are within ±0.4% of the calculated values.

Method 1: General Method for the Preparation of the Hydroxyguanidinium Derivatives. A mixture of the prepared cyanamide (1 equiv), predried hydroxylamine hydrochloride (4 equiv), and K_2CO_3 (8 equiv) in anhydrous EtOH containing 4 Å molecular sieves was prepared. This was stirred under argon overnight at room temperature. The reaction was monitored by TLC (MeOH/DCM, 1:7). The mixture was filtered through a pad of Celite using excess EtOH to complete the transfer. The product was concentrated under vacuum at ∼30 °C and used without further purification.

Method 2: General Method for the Preparation of Hydroxyguanidinium Hydrochloride Salts. The hydroxyguanidine free-base derivatives were treated with excess anhydrous 1 M HCl/ether solution overnight at room temperature. The product was concentrated under vacuum. Reverse-phase column chromatography was performed with the product eluting early with H_2O alone.

4,4′-Dihydroxyguanidiniumdiphenylmethane Dichloride (4a): Methods 1 and 2. Yellow solid (41%, 20% of total); mp,

dx.doi.org/10.1021/jm301358s | J. Med. Chem. 2013, 56, 451−459

decomposes over 180 °C; IR (ATR) 3682, 3322, 1619, 1603, 1579, 1510, 1432, 1416, 1298, 1246, 1206, 1182, 1109, 1077, 1019, 922, 872, 799, 767 cm^{-1}; ^1H NMR (D_2O) δ 3.96 (s, 2H, CH_2), 7.16 (d, 4H, J = 8.0 Hz, Ar), 7.28 (d, 4H, J = 8.0 Hz, Ar); ^{13}C NMR (400 MHz, D_2O) δ 39.7 (CH_2), 125.8, 129.8, 131.1, 141 (Ar), 157.4 (CN); HRMS (m/z, −ES) 315.1569 calcd [M^+ + H]; found 315.1563. Anal. ($C_{15}H_{20}Cl_2N_6O_2 \cdot 2.75H_2O$) C, H, N.

4,4′-Dihydroxyguanidiniumdiphenylether Dichloride (4b): Methods 1 and 2. Yellow solid (11% of total); mp, decomposes over 110 °C; IR (ATR) 3630, 3311, 1655, 1621, 1221, 1102, 910, 1499, 1406, 1286, 1167, 1077, 1014, 880, 862, 824 cm^{-1}; ^1H NMR (D_2O) δ 7.07 (d, 4H, J = 8.0 Hz, Ar), 7.25 (d, 4H, J = 8.0 Hz, Ar); ^{13}C NMR (400 MHz, D_2O) δ 119.7, 127.7, 128.5, 155.7 (Ar), 157.6 (CN); HRMS (m/z, −ES) 315.1362 calcd [M^+ + H]; found 317.1364. Anal. ($C_{14}H_{19}Cl_3N_6O_3 \cdot 2.5H_2O$) C, H, N.

4,4′-Dihydroxyguanidiniumdiphenylethylphenyl Dichloride (4c): Methods 1 and 2. Orange solid (21%, 11% of total); mp, decomposes over 165 °C; IR (ATR) 3671, 3414, 1658, 1590, 1565, 1514, 1496, 1451, 1420, 1404, 1371, 1304, 1243, 1096, 1051, 1018, 987, 824 cm^{-1}; ^1H NMR (D_2O) δ 2.9 (s, 4H, CH_2), 7.09 (d, 4H, J = 8.0 Hz, Ar), 7.21 (d, 4H, J = 8.0 Hz, Ar); ^{13}C NMR (400 MHz, D_2O) δ 35.9 (CH_2), 126.0, 130.1, 131.2, 141.9 (Ar), 158.0 (CN); HRMS (m/z, −ES) 329.1726 calcd [M^+ + H]; found 329.1732. Anal. ($C_{16}H_{22}Cl_2N_6O_4 \cdot 2H_2O$) C, H, N.

4,4′-Dihydroxyguanidiniumdiphenylthioether Dichloride (4d): Methods 1 and 2. Brown solid (27%, 19% of total); mp, decomposes over 247 °C; IR (ATR) 3692, 3301, 1651, 1611, 1591, 1568, 1515, 1490, 1405, 1344, 1302, 1274, 1244, 1179, 1108, 1080, 1014, 950, 904, 892, 862, 815, 736, 704, 672, cm^{-1}; ^1H NMR (D_2O) δ 7.18 (d, 4H, J = 8.0 Hz, Ar), 7.36 (d, 4H, J = 8.0 Hz, Ar); ^{13}C NMR (400 MHz, D_2O) δ 125.9, 131.9, 132.7, 133.8 (Ar), 156.9 (CN); HRMS (m/z, −ES) 333.1119 calcd [M^+ + H]; found 333.1134. Anal. ($C_{14}H_{19}Cl_3N_6O_2S \cdot 3H_2O$) C, H, N.

4,4′-Dihydroxyguanidiniumdiphenylcarbonyl Dichloride (4e): Methods 1 and 2. Yellow solid (23%, 8% of total); mp, decomposes over 115 °C; IR (ATR) 3748, 3370, 1662, 1646, 1623, 1593, 1564, 1558, 1511, 1449, 1389, 1372, 1318, 1293, 1282, 1248, 1182, 1145, 1080, 1015, 987, 975, 959, 934, 865, 850, 763, 738, 686, 667 cm^{-1}; ^1H NMR (D_2O) δ 7.34 (d, 4H, J = 8.0 Hz, Ar), 7.75 (d, 4H, J = 8.0 Hz, Ar); ^{13}C NMR (400 MHz, D_2O) δ 123. 2, 131.3, 134.0, 138.1 (Ar) 156.1 (CN), 197.39 (CO); HRMS (m/z, −ES) 329.1362 calcd [M^+ + H]; found 329.1361. Anal. ($C_{15}H_{18}Cl_2N_6O_3 \cdot 2.4H_2O$) C, H, N.

4,4′-Dihydroxyguanidiniumdiphenylamide Dichloride (4f): Methods 1 and 2. Off-white solid (14% of total); mp, decomposes over 190 °C; IR (ATR) 3646, 3178, 1652, 1627, 1602, 1549, 1515, 1475, 1412, 1340, 1298, 1243, 1180, 1120, 1077, 1019, 985, 904, 891, 844, 831, 812, 708, 656 cm^{-1}; ^1H NMR (D_2O) δ 7.32 (d, 4H, J = 8.0 Hz, Ar), 7.37 (d, 4H, J = 8.0 Hz, Ar) 7.57 (d, 4H, J = 8.0 Hz, Ar), 7.89 (d, 4H, J = 8.0 Hz, Ar); ^{13}C NMR (400 MHz, D_2O) δ 123.2, 124.3, 126.2, 128.8, 130.2, 132.0, 136.1, 137.3 (Ar), 156.7 (CN), 157.3 (CN), 168.3 (CO); HRMS (m/z, −ES) 344.1471 calcd [M^+ + H]; found 344.1461. Anal. ($C_{15}H_{19}Cl_2N_7O_3 \cdot 2H_2O$) C, H, N.

***N*-Phenylhydroxyguanidinium Hydrochloride (4g):[18] Methods 1 and 2.** Yellow oil (49%, 27% of total); IR (film) 3654, 3417, 1655, 1611, 1590, 1567, 1499, 1461, 1449,1390, 1341, 1314, 1298, 1249, 1196, 1181, 1156, 1119, 1068, 1032, 1004, 983, 966, 914, 943, 893, 842, 826, 795, 753, 694, 685 cm^{-1}; ^1H NMR (D_2O) δ 7.23 (d, 2H, J = 8.0 Hz, Ar), 7.27 (t, 1H, J = 8.0 Hz, Ar), 7.44 (t, 2H, J = 8.0 Hz, Ar), 7.96 (br s, 2H), 9.92 (br s, 1H), 10.11 (br s, 1H), 10.88 (br s, 1H); HRMS (m/z, −ES) 152.0824 calcd [M^+ + H]; found 152. 0823.

DNA Thermal Denaturation Assays. Thermal melting experiments were conducted with a Varian Cary 300 Bio spectrophotometer equipped with a 6 × 6 multicell temperature-controlled block. Temperature was monitored with a thermistor inserted into a 1 mL quartz cuvette containing the same volume of water as in the sample cells. Absorbance changes at 260 nm were monitored from a range of 20 to 90 °C with a heating rate of 1 °C per min and a data collection rate of five points per °C. The salmon sperm DNA was purchased from Sigma Aldrich (extinction coefficient ε_{260} = 6600 cm^{-1} M^{-1} base). A quartz cell with a 1 cm path length was filled with a 1 mL solution of DNA polymer or DNA compound complex. The DNA polymer (150 μM base) and the compound solution (15 μM) were prepared in a phosphate buffer [0.01 M Na_2HPO_4/NaH_2PO_4], adjusted to pH 7, so that a compound to DNA base ratio of 0.1 was obtained. The thermal melting temperatures of the duplex or duplex-compound complex obtained from the first derivative of the melting curves are reported.

Biochemistry. Cell Culture. Human Caucasian promyelocytic leukemia HL-60 and MCF-7 human breast carcinoma breast cells were obtained from the European Collection of Cell Culures (Porton Down, Wiltshire, U.K.). Neuroblastoma Kelly cells were a kind gift from the Royal College of Surgeons (St. Stephens Green, Dublin 2, Ireland). HL-60 and Kelly cells were grown in Roswell Park Memorial Institute (RPMI) 1640 medium with GlutaMax I supplemented with 10% (v/v) fetal bovine serum (FBS) and 50 μg mL^{-1} penicillin/streptomycin (pen−strep). MCF-7 cells were grown in minimum essential medium (MEM) with GlutaMax I supplemented with 10% (v/v) FBS, 1% nonessential MEM amino acids, and 50 μg mL^{-1} pen−strep. Cells were grown at 37 °C in a humidified environment maintained at 95% O_2 and 5% CO_2 and passaged at least twice weekly (HL-60) or once weekly (Kelly, MCF-7) depending on their levels of confluency. HL-60 cells were maintained at a density of between 2 × 10^5 and 2 × 10^6 cells/mL. Adherent cells (Kelly cells and MCF-7) were subcultured by trypsinization upon reaching 90% confluency.

Compound Preparation. Stock solutions (10 mM) of the compounds were prepared in sterile ddH_2O and were then sterile filtered (0.2 μM filters). Required concentration ranges (10−0.1 mM) of each drug were prepared in sterile ddH_2O and stored at −20 °C until required.

Cell Viability (AlamarBlue Assays). HL-60 cells in the log phase of growth were seeded in 96-well plates at a density of 200 000 cells mL^{-1} (200 μL/well or 40 000 cells/well) in complete RPMI medium. The cells were then treated with a 1:100 dilution of stock concentrations of drugs in triplicate. Three blank wells containing 200 μL of RPMI were set up as blanks. MCF-7 cells were seeded at a density of 50 000 cells mL^{-1} (200 μL/well or 10 000/well) and Kelly cells at 30 000 cells mL^{-1} (200 μL/well or 6000/well) and incubated at 37 °C for 24 h. The cells were then treated with the drugs as for the HL-60 cells. After 72 h of incubation, 20 μL of AlamarBlue was added to each well. The plates were incubated in darkness at 37 °C for 4.5 h. By use of a Molecular Devices microplate reader, the fluorescence (F) was then read at an excitation wavelength of 544 nm and an emission wavelength of 590 nm. Cell viability was then determined by subtracting the mean blank fluorescence (F_b) from the treated sample fluorescence (F_s) and expressing this as a percentage of the fluorescence of the blanked vehicle control (F_c), as shown in eq 1.

$$\frac{F_s - F_b}{F_c - F_b} \times 100 = \%\ \text{cell viability} \quad (1)$$

The results were then plotted as nonlinear regression, sigmoidal dose−response curves on Prism, from which the IC_{50} value for each drug was determined.

Determination of DNA Content (Flow Cytometry) of HL-60 Cells. HL-60 cells were seeded at 200 000 cells mL^{-1} in T25 flasks and treated with appropriate drug concentrations or ddH_2O as vehicle control for 24, 48, or 72 h. Cells were harvested at each time-point by centrifugation at 300g for 8 min and the pellets resuspended in 200 μL of nonsterile PBS. The cells were then fixed by a dropwise addition of 2 mL of ice-cold 70% EtOH/PBS while gently being vortexed. Following overnight fixation at −20 °C, 10 μL of nonsterile FBS was added to the cells and the solutions were centrifuged at 800g for 10 min. Ethanol was then drained, the cell pellet resuspended in PBS containing 0.5 mg mL^{-1} RNase-A (to denature RNA) and 0.15 mg mL^{-1} propidium iodide (PI, a fluorescent DNA binding dye) and then incubated in the dark at 37 °C for 30 min. The PI fluorescence was measured on a linear scale using a FACS Calibur flow cytometer (Becton Dickinson, San Jose, CA). Data collections (10 000 events per sample) were gated to exclude cell debris and cell aggregates. The

dx.doi.org/10.1021/jm301358s | J. Med. Chem. 2013, 56, 451−459

amount of fluorescence is proportional to the amount of DNA present, and hence, the population of cells in each phase of the cell cycle can be determined. Cells are gated as follows: M1 = pre-G_1 (<2N DNA), M2 = G_0/G_1 (2N DNA), M3 = S (2N−4N DNA), M4 = G_2/M (4N DNA), M5 = (G_n > 4N DNA). Apoptotic cells are hypoploid (<2N DNA). Therefore, apoptosis was determined from the peak in M1. All data were recorded and analyzed using the CellQuest software (Becton Dickinson, San Jose, CA).

Statistical Analysis. Results were presented as the mean ± SEM. The statistical analysis of experimental data was performed using Prism GraphPad 4. *P* values were determined using a two-tailed Student's unpaired *t* test. $P < 0.05$ was considered to be significant.

■ ASSOCIATED CONTENT

Supporting Information

Preparation of the CbzNCS precursor (**1**) and the protected hydroxyguanidinium intermediates (**2a** and **2b**), ^{1}H and ^{13}C NMR characterization data of the cyanamide intermediates (**5a**−**f**) and the new target compounds (**4a**−**f**), and table listing combustion analysis data for these target compounds. This material is available free of charge via the Internet at http://pubs.acs.org.

■ AUTHOR INFORMATION

Corresponding Author

*Phone: +353 1 608 3731. Fax: +353 1 671 2826. E-mail: rozasi@tcd.ie.

Notes

The authors declare no competing financial interest.

■ ACKNOWLEDGMENTS

This research was funded by the SFI-RFP Project CHE275.

■ ABBREVIATIONS USED

MGB, minor groove binder; DNA, deoxyribonucleic acid; HB, hydrogen bond; HL-60, human promyelocytic; MCF-7, breast carcinoma; IC_{50}, concentration required for 50% inhibition

■ REFERENCES

(1) *Cancer*; Fact Sheet No. 297; World Health Organization: Geneva, Switzerland; http://www.who.int/mediacentre/factsheets/fs297/en/index.html.

(2) Sporn, M. B. The war on cancer. *Lancet* **1996**, *347*, 1377−1381.

(3) Thurston, D. E. *Chemistry and Pharmacology of Anticancer Drugs*; CRC Press/Taylor and Francis Group: Boca Raton, FL, 2007.

(4) Dudouit, F.; Goossens, J.-F.; Houssin, R.; Hénichart, J.-P.; Colson, P.; Houssier, C.; Gelus, N.; Bailly, C. Synthesis, DNA binding, topoisomerases inhibition and cytotoxic properties of 4-arylcarboxamidopyrrolo-2-carboxyanilides. *Bioorg. Med. Chem. Lett.* **2000**, *11*, 553−557.

(5) Rodríguez, F.; Rozas, I.; Kaiser, M.; Brun, R.; Nguyen, B.; Wilson, D.; Garcia, R. N.; Dardonville, C. New bis-(2-aminoimidazoline) and bisguanidine DNA minor groove binders with potent in vivo antitrypanosomal and antiplasmodial activity. *J. Med. Chem.* **2008**, *51*, 909−923.

(6) Nagle, P. S.; Rodríguez, F.; Kahvedžić, A.; Quinn, S. J.; Rozas, I. Asymmetrical diaromatic guanidinium/2-aminoimidazolinium derivatives: synthesis and DNA affinity. *J. Med. Chem.* **2009**, *52*, 7113−7121.

(7) Nagle, P. S.; Quinn, S. J.; Kelly, J. M.; O'Donovan, D. H.; Khan, A. R.; Rodríguez, F.; Nguyen, B.; Wilson, W. D.; Rozas, I. Understanding the DNA binding of novel non-symmetrical guanidinium/2-aminoimidazolinium derivatives. *Org. Biomol. Chem.* **2010**, *8*, 5558−5567.

(8) Goonan, A.; Kahvedžić, A.; Rodríguez, F.; Nagle, P. S.; McCabe, T.; Rozas, I.; Erdozain, A. M.; Meana, J. J.; Callado, L. F. Novel synthesis and pharmacological evaluation as α2-adrenoceptor ligands of *O*-phenylisouronium salts. *Bioorg. Med. Chem.* **2008**, *16*, 8210−8217.

(9) Hong, W. K., Bast, R. C., Hait, W., Kufe, D. W., Holland, J. F., Pollock, R. E., Weichselbaum, R. R., Eds. *Holland Frei Cancer Medicine 8*, 8th ed.; People's Medical Publishing House: Shelton, CT, 2010; p 2021.

(10) Adamson, R. H. Hydroxyguanidine—a new antitumour drug. *Nature* **1972**, *236*, 400−401.

(11) Young, C. W.; Schochetman, G.; Hodas, S.; Balis, M. E. Inhibition of DNA synthesis by hydroxyurea: structure−activity relationships. *Cancer Res.* **1967**, *27*, 535−540.

(12) Stella, V. J., et al.et al., Eds. *Prodrugs: Challenges and Rewards*: Springer: New York, 2007; Part 1, p 193.

(13) Boykin, D. W.; Kumar, A.; Hall, J. E.; Bender, B. C.; Tidwell, R. R. Anti-pneumocystis activity of bis-amidooximes and bis-*o*-alkylamidooximes prodrugs. *Bioorg. Med. Chem. Lett.* **1996**, *6*, 3017−3020.

(14) Martin, N. I.; Woodward, J. J.; Marletta, M. A. NG-Hydroxyguanidines from primary amines. *Org. Lett.* **2006**, *8*, 4035−4038.

(15) Linton, B. R.; Carr, A. J.; Orner, B. P.; Hamilton, A. D. A versatile one-pot synthesis of 1,3-substituted guanidines from carbamoyl isothiocyanates. *J. Org. Chem.* **2000**, *65*, 1566−1568.

(16) Orner, B. P.; Hamilton, A. D. The guanidinium group in molecular recognition: design and synthetic approaches. *J. Inclusion Phenom. Macrocyclic Chem.* **2001**, *41*, 141−147.

(17) Kiso, Y.; Ukawa, K.; Akita, T. Efficient removal of *N*-benzyloxycarbonyl group by a "push−pull" mechanism using thioanisole-trifuoroacetic acid, exemplified by a synthesis of Met-enkephalin. *J. Chem. Soc., Chem. Commun.* **1980**, *3*, 101−102.

(18) Bailey, D. M.; DeGrazia, C. G.; Lape, H. E.; Frering, R.; Fort, D.; Skulan, T. Hydroxyguanidines. New class of antihypertensive agents. *J. Med. Chem.* **1973**, *16*, 151−156.

(19) Renodon-Corniere, A.; Dijols, S.; Perollier, C.; Lefevre-Groboillot, D.; Boucher, J. L.; Attias, R.; Sari, M. A.; Stuehr, D.; Mansuy, D. *N*-Aryl *N*′-hydroxyguanidines, a new class of NO-donors after selective oxidation by nitric oxide synthases: structure−activity relationship. *J. Med. Chem.* **2002**, *45*, 944−954.

(20) Slama, P.; Boucher, J.-L.; Reglier, M. Aromatic *N*-hydroxyguanidines as new reduction cosubstrates for dopamine β-hydroxylase. *Biochem. Biophys. Res. Commun.* **2004**, *316*, 1081−1087.

(21) Xian, M.; Fujiwara, N.; Wen, Z.; Cai, T.; Kazuma, S.; Janczuk, A. J.; Tang, X.; Telyatnikov, V. V.; Zhang, Y.; Chen, X.; Miyamoto, Y.; Taniguchi, N.; Wanga, P. G. Novel substrates for nitric oxide synthases. *Bioorg. Med. Chem.* **2002**, *10*, 3049−3055.

(22) Pankratov, V. A.; Korshak, V. V.; Vinogradova, S. V.; Antsiferova, N. P.; Kutepov, D. F. Synthesis of aromatic cyanamides. *Russ. Chem. Bull.* **1975**, *24*, 2198−2199.

(23) Nekrasov, D. D. Synthesis and chemical transformations of mono and disubstituted cyanamides. *Russ. J. Org. Chem.* **2004**, *40*, 1439−1454.

(24) Olofson, R. A.; Pepe, J. P. *N*-Cyanamidopyrroles and *N*-cyanamidoimines from 4-amino-1,2,4-triazole. *Tetrahedron Lett.* **1979**, *20*, 3129−3130.

(25) Cai, T.; Xian, M.; Wang, P. G. Electrochemical and peroxidase oxidation study of *N*′-hydroxyguanidine derivatives as NO donors. *Bioorg. Med. Chem. Lett.* **2002**, *12*, 1507−1510.

(26) Schade, D.; Klein, N.; Kotthaus, J.; Clement, B. Prodrug design for the potent cardiovascular agent *N*-hydroxy-L-arginine (NOHA): synthetic approaches and physicochemical characterization. *Org. Biomol. Chem.* **2011**, *9*, 5249−5259.

(27) Nagle, P. S.; Rodriguez, F.; Nguyen, B.; Wilson, W. D.; Rozas, I. High DNA affinity of a series of amide linked aromatic dications. *J. Med. Chem.* **2012**, *55*, 4397−4406.

(28) Dardonville, C.; Barrett, M. P.; Brun, R.; Kaiser, M.; Tanious, F.; Wilson, W. D. DNA binding affinity of bisguanidine and bis(2-aminoimidazoline) derivatives with in vivo antitrypanosomal activity. *J. Med. Chem.* **2006**, *49*, 3748−3752.

(29) Glass, L. S.; Nguyen, B.; Goodwin, K. D.; Dardonville, C.; Wilson, W. D.; Long, E. C.; Georgiadis, M. M. Crystal structure of a

trypanocidal 4,4′-bis-(imidazolinylamino)diphenylamine bound to DNA. *Biochemistry* **2009**, *48*, 5943−5952.
(30) Berger, B. J.; Lombardy, R. J.; Marbury, G. D.; Bell, C. A.; Dykstra, C. C.; Hall, J. E.; Tidwell, R. R. Metabolic *N*-hydroxylation of pentamidine in vitro. *Antimicrob. Agents. Chemother.* **1990**, *34*, 1678−1684.
(31) Perrin, D. D. *Dissociation Constants of Organic Bases in Aqueous Solution*; Butterworths, London, 1965; Supplement, 1972.
(32) Nagle, P. S.; Kahvedžić, A.; McCabe, T.; Rozas, I. On the protonated state of amidinium-like diaromatic derivatives: X-ray and UV studies. *Struct. Chem.* **2011**, 1−9.
(33) Voytik-Harbin, S. L.; Brightman, A. O.; Waisner, B.; Lamar, C. H.; Badylak, S. F. Application and evaluation of the alamarBlue assay for cell growth and survival of fibroblasts. *In Vitro Cell. Dev. Biol.: Anim.* **1998**, *34*, 239−246.
(34) Nakayama, G. R.; Caton, M. C.; Nova, M. P.; Parandoosh, Z. Assessment of the Alamar Blue assay for cellular growth and viability in vitro. *J. Immunol. Methods* **1997**, *24*, 205−208.
(35) Jiang, J. F.; Liu, W. J.; Ding, J. Regulation of telomerase activity in camptothecin-induced apoptosis of human leukemia HL-60 cells. *Acta Pharmacol. Sin.* **2000**, *21*, 759−764.
(36) Hiraku, Y.; Oikawa, S.; Kawanishi, S. Distamycin A, a minor groove binder, changes enediyne-induced DNA cleavage sites and enhances apoptosis. *Nucleic Acids Res., Suppl.* **2002**, *2*, 95−96.
(37) (a) Lansiaux, A.; Dassonneville, L.; Facompre, M.; Kumar, A.; Stephens, C. E.; Bajic, M.; Tanious, F.; Wilson, W. D.; Boykin, D. W.; Bailly, C. Distribution of furamidine analogues in tumor cells: influence of the number of positive charges. *J. Med. Chem.* **2002**, *45*, 1994−2002. (b) Ekelund, S.; Nygren, P.; Larsson, R. Guanidino-containing drugs in cancer chemotherapy: biochemical and clinical pharmacology. *Biochem. Pharmacol.* **2001**, *61*, 1183−1193. (c) Lansiaux, A.; Tanious, F.; Mishal, Z.; Dassonneville, L.; Kumar, A.; Stephens, C. E.; Hu, Q.; Wilson, W. D.; Boykin, D. W.; Bailly, C. Distribution of furamidine analogues in tumor cells: targeting of the nucleus or mitochondria depending on the amidine substitution. *Cancer Res.* **2002**, *62*, 7219−7229.
(38) Kahvedžić, A.; Zisterer, D.; Rozas, I. Unpublished results.
(39) Lansiaux, A.; Tanious, F.; Mishal, Z.; Dassonneville, L.; Kumar, A.; Stephens, C. E.; Hu, Q.; Wilson, W. D.; Boykin, D. W.; Bailly, C. Distribution of furamidine analogues in tumor cells: targeting of the nucleus or mitochondria depending on the amidine substitution. *Cancer Res.* **2002**, *62*, 7219−7229.
(40) The pK_a values were calculated by means of UV−vis titrations. Thus, protonation of a solution of the compound with HCl acid was followed by titration with aliquots of base (NaOH, 0.1 M). With each subsequent addition, the pH value was measured and the corresponding UV spectrum recorded accordingly. Changes of the UV spectrum were monitored over a wide range of pH values.
(41) Ming, X.; Ju, W.; Wu, H.; Tidwell, R. R.; Hall, J. E.; Thakker, D. R. *Drug Metab. Dispos.* **2009**, *37*, 424−430.
(42) Thiele, C. J. *Neuroblastoma in Human Cell Culture*.; Kluwer Academic Publishers: Dordrecht, The Netherlands, 1998; Vol. *1*, pp 21−53.